Available online at www.sciencedirect.com
ScienceDirect
Journal of Power Sources 162 (2006) 851–863
JOURNAL OF POWER SOURCES
www.elsevier.com/locate/jpowsour

Studies on electrolyte formulations to improve life of lead acid batteries working under partial state of charge conditions

J.C. Hernández, M.L. Soria *, M. González, E. García-Quismondo, A. Muñoz, F. Trinidad

Exide Technologies, Research and Innovation, Autovía A-2, km 42, E-19200 Azuqueca de Henares, Spain

Received 11 February 2005; accepted 15 July 2005
Available online 19 September 2005

Abstract

For decades, valve regulated lead acid batteries with gel electrolyte have proved their excellent performance in deep cycling applications. However, their higher cost, when compared with flooded batteries, has limited their use in cost sensitive applications, such as automotive or PV installations.

The use of flooded batteries in deep or partial state of charge working conditions leads to limited life due to premature capacity loss provoked by electrolyte stratification. Different electrolyte formulations have been tested, in order to achieve the best compromise between cost and life performance. Work carried out included electrochemical studies in order to determine the electrolyte stability and diffusional properties, and kinetic studies to check the processability of the electrolyte formulation. Finally, several 12 V batteries have been assembled and tested according to different ageing profiles.

Keywords: Valve-regulated lead-acid batteries; Gel electrolytes; PSOC; Cycle life; Failure mode analysis

1. Introduction

Flooded lead-acid batteries are now extensively used in automotive as well as in many traction and stationary applications, due to their lower cost when compared to valve regulated lead acid (VRLA) batteries, either with gel or absorptive glass mat (AGM) technologies.

However, novel vehicle requirements demand battery working regimes mainly under partial-state-of-charge (PSOC) conditions, that, in the case of flooded batteries, lead to premature capacity loss provoked by electrolyte stratification [1]. Changes in the demands on automotive batteries [2] are caused by the increase of on-board power requirements due to the introduction of several new features, such us the replacement of mechanical by electrical functions (steer- and brake-by-wire, air conditioning, ...) to provide enhanced safety and comfort, as well as of novel functions (Stop and Start, regenerative braking, etc.) aimed at achieving significant fuel consumption and emission savings [3].

According to the power requirements and vehicle hybridisation degree, several drivetrain and powernet architectures have been proposed [4], with nominal voltages ranging from 14 to nearly 300 V in automobiles and over 600 V in hybrid buses. Moreover, different electrochemical systems have been installed either in commercial hybrid vehicles or in demonstration prototypes: the well known hybrid vehicles Toyota Prius, Honda Insight or Ford Escape, with high voltage Ni-MH batteries, the Citröen C3 with Stop and Start function and an AGM VRLA 12 V battery, and the Nissan Tino with a Li-ion 346 V battery [5].

VRLA batteries are today the cost effective solution for short term low voltage applications (14–42 V powernets), due to their availability, cost and low temperature performance. AGM technology is commonly used, due to the high power capability demanded as well as to the improved life when compared with flooded designs and its intrinsic maintenance

* Corresponding author. Tel.: +34 949 263 316; fax: +34 949 262 560.
E-mail address: soriaml@tudor.es (M.L. Soria).

0378-7753/$ – see front matter © 2005 Elsevier B.V. All rights reserved.
doi:10.1016/j.jpowsour.2005.07.042

free characteristics. However, as the electrolyte is limited to that absorbed in the separator, extensive cycling can lead to battery dry-out and even to thermal runaway.

On the other hand, gel batteries have up to date been the preferred choice for deep cycling applications, as electrolyte immobilisation hinders somewhat its stratification and thus premature irreversible sulphation of active materials [6]. However, their power capability is limited by the higher electrolyte internal resistance and by the use of thick plate designs in commercial applications (products for deep cycling).

Within the Supercar project [7], some car manufacturers are testing hybrid configurations for the energy storage system, so that energy generated during vehicle brake is recovered by a high power device (a double layer capacitor, also known as supercapacitor), whereas the battery provides energy to all the consumers during vehicle stops and regen and boost phases [3]. In this case, the battery should be characterised by a long-lasting life under moderate rate (around 1–2 C A discharge and charge) conditions. For this reason, gel type batteries with electrode design and active materials adapted to automotive applications have been extensively studied for these hybrid energy storage configurations. Different gel formulations have been tested in order to obtain the best performance compromise between initial performance (capacity and cold cranking) and life under different moderate rate PSOC conditions.

2. Experimental

2.1. Electrolyte preparation

Several gel formulations were prepared using sulphuric acid and different inorganic commercial compounds, mainly with a silica basis. Table 1 summarises the main characteristics of the commercial gelators used in these investigations. As shown, one of the key parameters is the BET specific surface, related to the particle size, which will control the gelation kinetics and the final gel strength [8]. Another important parameter is the doping content: the SiO_2 is doped with different percentages of aluminium in order to modify the siloxane bond strength.

Two sulphuric acid concentrations have been studied in the electrochemical experiments: 1.285 and 1.300 g cm^{-3}, whereas in the prototypes assembled with gel electrolyte, only the latter concentration was used. Electrolytes containing fumed silica were prepared by mixing the cooled 1.300 g cm^{-3} sulphuric acid (−5 °C) with the inorganic compound during 10 min with a high speed mixer at 8000 rpm. On the other hand, electrolytes containing colloidal silica were prepared by mixing the cooled sulphuric acid with a low speed mixer during 4 min. In this case, H_2SO_4 concentration was calculated to become 1.300 g cm^{-3} after dilution with the silica colloid. All the formulations included 15 g l^{-1} of Na_2SO_4 and 3 g l^{-1} $MgSO_4$ as additives to improve the battery rechargeability at low state of charge (SOC).

The electrolyte formulations to be tested in batteries were chosen taking into account the final gel characteristics (stability and strength) and the gelling time. Gelling time is a process parameter that affects the electrolyte processability during battery assembly (filling and formation). An optimum compound would maintain its liquid characteristics till the end of the battery manufacturing processes and then would gellify.

With the aim of determining the gelling time of the silica compounds, a kinetic study was carried out by measuring the penetration of lead balls (3 mm diameter) into the gel at different times. SiO_2 concentration, acid concentration and initial temperature were variables studied in this investigation. These results can be summarised:

- Increasing the acid concentration, the gelling time is shorter.
- Increasing the silica concentration, the gelling time is shorter. However, it is necessary a minimum SiO_2 content to obtain a good gel structure [8].
- It is possible to reduce the gelling rate by reducing the initial acid temperature.
- Using silica-based compounds with smaller particle size (higher BET), the gelling rate is increased.
- Generally, colloidal silica compounds need less time to form the gel structure (duration) than fumed silica compounds.

In this way, several electrolyte formulations were selected to be tested in batteries.

2.2. Electrochemical experiments

In order to evaluate the electrochemical performance of the commercial silica compounds, cyclic and linear voltammetry

Table 1
Main characteristics of different commercial gel forming compounds

Sample	SiO_2 (%)	Al_2O_3 (%)	TiO_2 (%)	BET (m^2 g^{-1})	Particle size (nm)	
A	>99.8	<0.05	<0.03	200 ± 25	12	Fumed silica
B	>99.8	<0.05	<0.03	300 ± 30	7	Fumed silica
C	>99.8	<0.05	<0.03	380 ± 30	7	Fumed silica
D	>98.3	0.3–1.3	<0.03	170 ± 30	15	Fumed silica with Al
E	82–86	14–18	<0.03	170 ± 30	NA	Alumino silicate
F	15	Al 130 (ppm)	Ti 35 (ppm)	750	4	Colloidal silica
G	40	Al 230 (ppm)	Ti 40 (ppm)	250	14	Colloidal silica

techniques and electrochemical impedance spectroscopy (EIS) were used.

The voltammetric experiments were carried out using a conventional three electrode system. The cell was filled with the electrolyte just after preparation (liquid state) and argon was blown into the electrolyte with the aim of removing all the oxygen from the solution. Afterwards, 24 h rest were required to assure the complete gel formation.

Cyclic voltammetry studies were carried out with a EG&G Princeton Applied Research Potentiostat/Galvanostat Model 263 A, at different scan rates (from 5 to 200 mV s^{-1} and between 1.9 and −1.9 V versus MSE) for all the gel electrolytes, using an electrochemical cell with lead working (WE) and counter (CE) electrodes and a mercurous sulphate electrode (MSE) ($Hg/HgSO_4/H_2SO_4$) as reference electrode (RE). All the experiments were performed at room temperature of 20 °C. Before every measurement the WE was polarised at –1.8 V versus MSE during 10 min.

Linear voltammetry experiments were carried out from the equilibrium state to −2.2 V versus MSE in the cathodic sweep and to 2.3 V versus MSE in the anodic sweep, at 20 mV s^{-1}. In order to simulate the battery behaviour, stabilised Pb° (by 10 min polarisation at −1.8 V versus MSE) for the cathodic sweep and PbO_2 (obtained by anodic polarisation at 1.3 V versus MSE of a Pb electrode for 3 h) for the anodic sweep were used as WE.

Finally, EIS measurements were performed with a EIS-meter equipment, version 1.2 with 14 channels, developed by RWTH-ISEA. Spectra acquisition was carried out directly on a 12 V 18 Ah battery at different SOC from 10,000 Hz to 0.003937 Hz.

2.3. Battery testing

Several battery prototypes were assembled using standard polypropylene containers sized 175 mm × 80 mm × 174 mm, dry charged plates prepared with standard gravity casted grids, automotive standard positive and negative active material formulations and phenolic resin leaf separators. On the other hand, 12 V AGM prototype batteries were assembled with standard ABS containers sized 180 mm × 75 mm × 150 mm, which are commonly used in the manufacture of 15 Ah gel VRLA batteries for stand-by applications. The battery design was based on former work on the development of high power VRLA batteries for UPS applications [9], and was characterised by thin plate technology (around 1 mm thickness) and the use as separator of a combination of absorptive glass mat (AGM) material and a microporous polyethylene membrane to avoid premature battery failure due to shortcircuits.

Batteries were filled with different electrolyte formulations using a vacuum system to improve the gel distribution. Batteries with resin separators were filled with the gel formulations selected in the kinetic study, however, AGM prototypes were filled with a low concentration colloidal silica based gel: AGM materials absorb part of the sulphuric acid, increasing the silica concentration in the rest of the electrolyte.

Electrical testing of the batteries was carried out with computer controlled cycling equipment: Bitrode LCN-7-100-12 and Digatron UBT 100-20-6BTS. High rate discharges were performed with a computer controlled Digatron UBT BTS-500 mod. HEW 2000-6BTS.

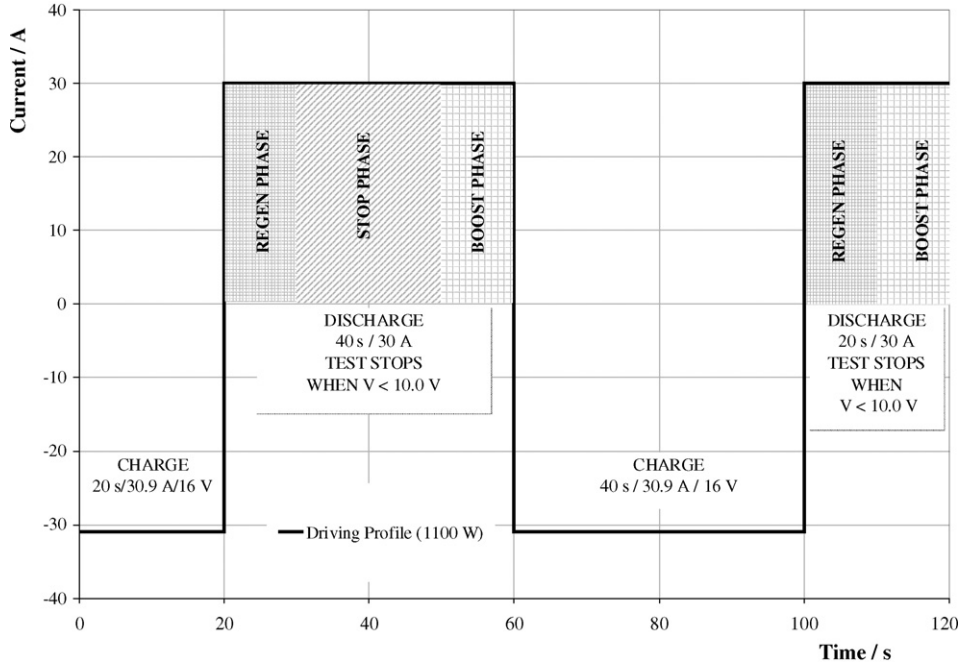

Fig. 1. Battery testing conditions according to Stop and Start profile.

Tests of gel batteries included initial capacity, high rate and cold cranking checks as well as cycle life performance under PSOC and low-moderate rate conditions (50% SOC, 17.5% depth of discharge (DOD) and C/3 A). Moreover, a specific profile that simulates battery working conditions in a vehicle designed with the Stop and Start and regenerative braking functions and equipped with integrated starter generator and a supercapacitor for peak power capability, and described formerly [10] has also been tested. According to this profile (Fig. 1), that corresponds to a total in-vehicle consumption of 1100 W, tests were carried out with a charge and discharge rates of nearly 2C and at 2% DOD and 80% SOC. A capacity check and a recharge (4.5 A/14.4 V/12 h + 0.45 A/4 h) were carried out every 10,000 microcycles. Moreover, the batteries were recharged every 500 microcycles at 16 V/30 A during one hour to compensate the capacity loss due to the limited charge conditions of the proposed working profile.

After the cycle life test, batteries were torn down to determine the failure mode. Chemical analyses of the active material samples were carried out using internal volumetric (PbO_2) and gravimetric ($PbSO_4$) procedures. Active material porosity was measured with a mercury intrusion porosimeter Micromeritics Autopore 9405 and specific surface (BET) with a Micromeritics FlowSorb II 2300. Morphological studies have been carried out by scanning electron microscopy.

3. Results and discussion

3.1. Electrochemical study

Fig. 2 shows a comparison of several gel composition and acid electrolytes. No additional peaks appear in the voltammograms of any of the new gel compositions due to secondary redox reactions of the silica compounds, only an adsorption capacity plateau in some cases (fumed silica) at more anodic potentials than the Pb/Pb^{2+} transition. This fact confirms that all the silica based gelators studied are stable in the operative conditions of the battery.

As it can be observed in Fig. 3, slight redox potential (E_P) shifts appear when a silica compound is added to the sulphuric acid. On the other hand, differences in the intensity of the redox peaks (i_P) appear when comparing acid and gel electrolytes [11]. This effect is more significant at high scan rates and it could be attributed to the fact that the silica adsorbs the polar ions (H^+ and $SO_4{}^{2-}$) reducing their activity [12] and, on the other hand, the three dimensional gel structure hinders the ion diffusion.

In this way, the change in the E_P and i_P values with regard to the scan rate for the discharge process (transition $Pb^\circ/PbSO_4$), implies that the reaction can not be considered reversible in this range of scan rates [13].

Consequently, the equations will be for an irreversible process:

$$i_P = (2.99 \times 10^5) n(\alpha n_a)^{1/2} D_o^{1/2} C_o^* V^{1/2}$$

$$E_P = E^{o'} - \frac{RT}{\alpha n_a F} \times \left(0.780 + \ln\left(\frac{D_o^{1/2}}{k^o}\right) + \ln\left(\frac{\alpha n_a F V}{RT}\right)^{1/2}\right)$$

where i_P is the peak density current, n is the number of electrons per molecule oxidised or reduced, α is the transfer coefficient, n_a is the number of electrons involved in the rate determining step (rds), V is the linear potential scan rate, C_o^* is the acid concentration, D_o is the diffusion coefficient, F is the Faraday, R the gas constant, T the temperature, k^o the standard heterogeneous rate constant, $E^{o'}$ the formal potential of the electrode and E_P the peak potential.

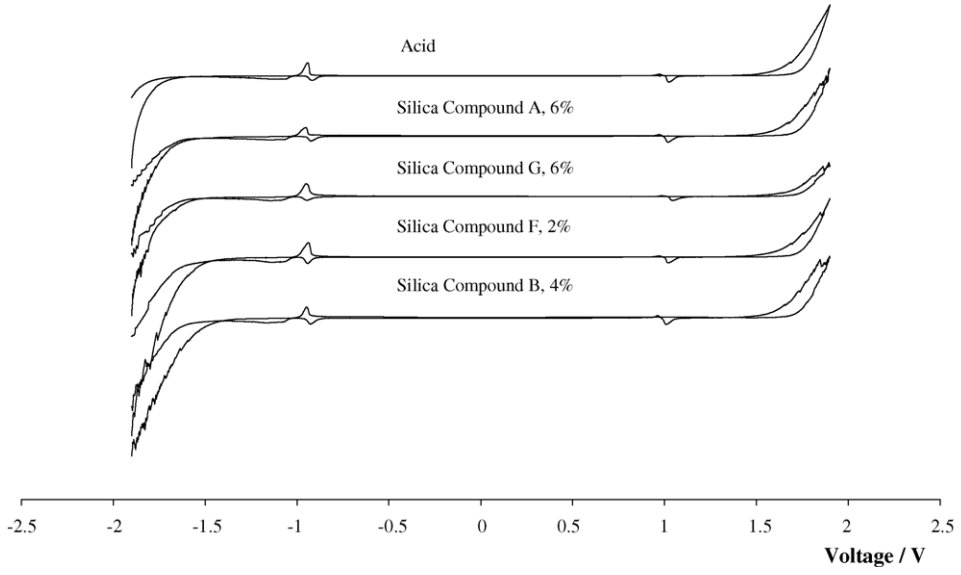

Fig. 2. Cyclic voltammogram of a Pb WE in different electrolytes at 20 mV s^{-1}.

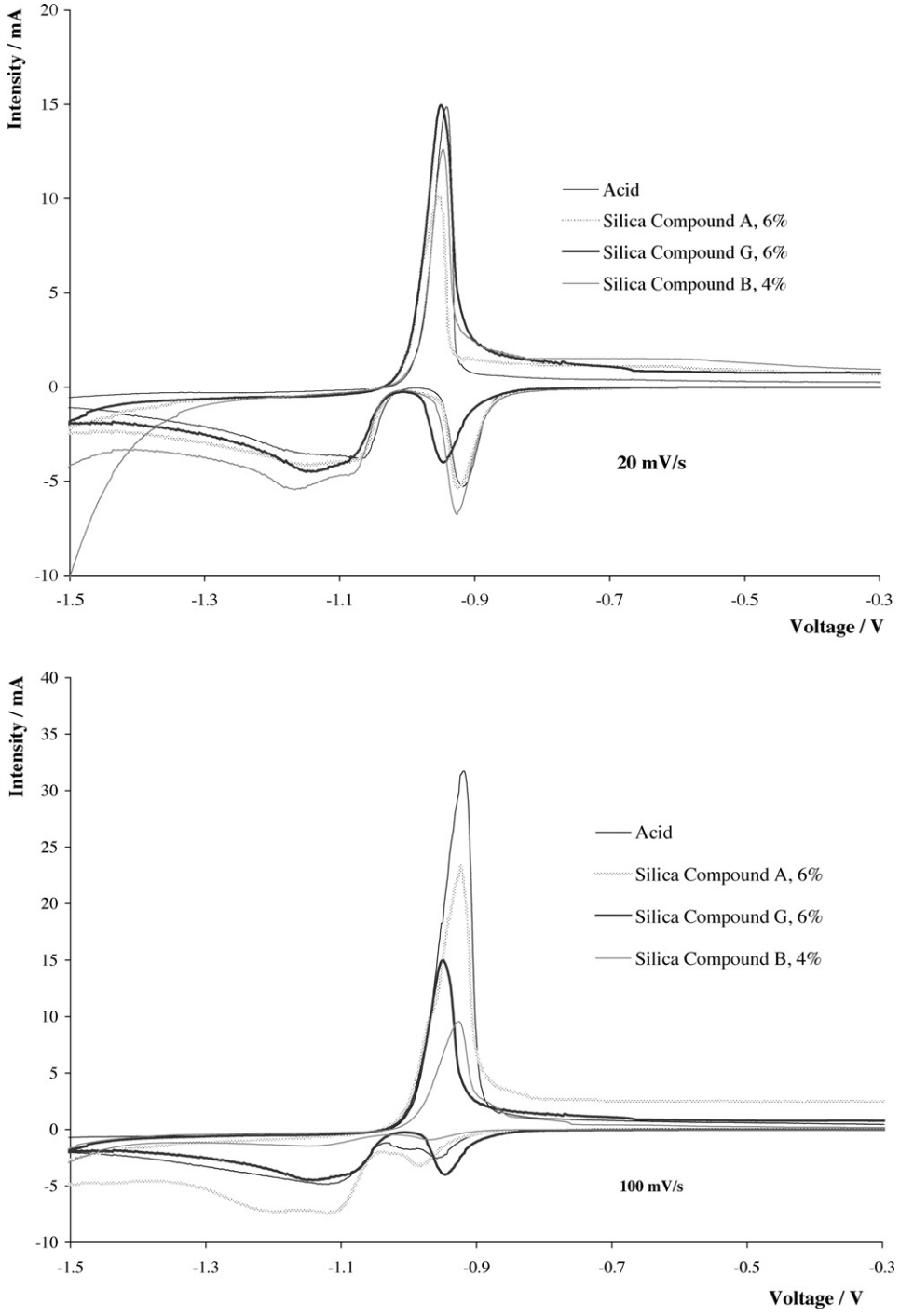

Fig. 3. Cyclic voltammogram of a Pb WE in different electrolytes at 20 and 100 mV s^{-1}.

Thus, the ratio i_P versus $V^{1/2}$ is proportional to the diffusion coefficient D_o of the electrochemical system. Fig. 4 shows the anodic peak intensity represented versus the square root of the scan rate for different gel electrolytes and a standard acid electrolyte. Therefore, if only the electrolyte is changed in the electrochemical cell and the experimental conditions are fixed, the differences in the slopes are only related to a change in the diffusion coefficient. On adding a silica compound to the electrolyte, a three dimensional structure is created that limits the ion diffusion, decreasing the D_o of the system.

Gel electrolytes with a very open structure, like colloidal silica based gels, show slopes (proportional to D_o) closer to the sulphuric acid, and thus a lower decrease in the capacity and in the high rate performance when compared to the liquid electrolyte are obtained.

Other important effect provoked by the gel electrolyte, is the shift of oxygen and hydrogen overpotentials, that can be

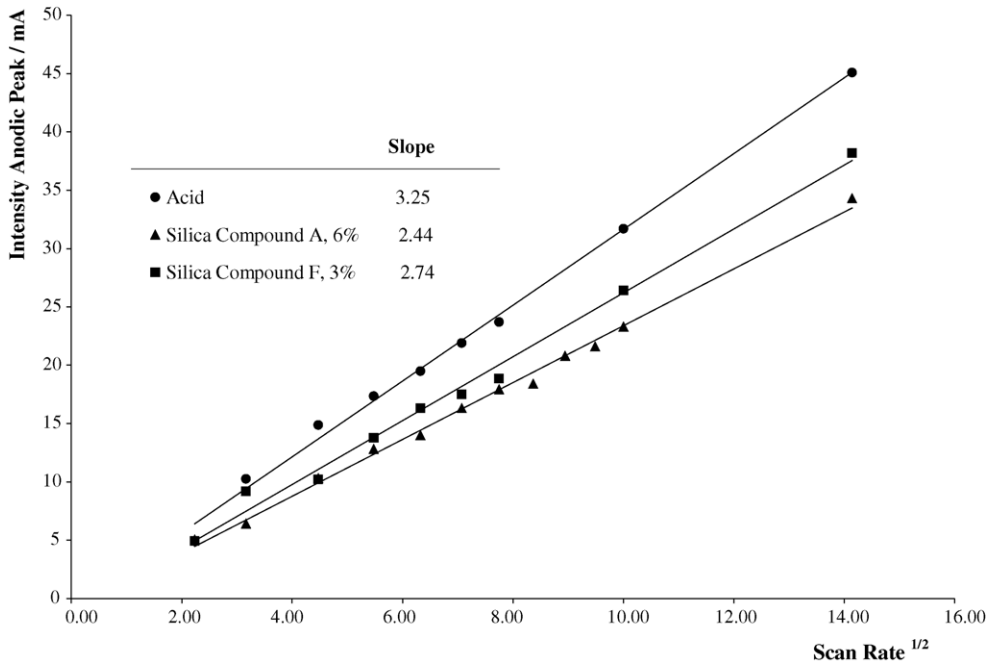

Fig. 4. Dependence of anodic peak intensity with scan rate$^{1/2}$ for different gel electrolytes.

studied by linear voltammetry for the cathodic and anodic sweeps using a Pb WE and a PbO_2 WE, respectively.

Fig. 5 shows the cathodic Tafel plots (H_2 evolution) of some gel formulations (examples of sulphuric acid, fumed silica and colloidal silica) compared to a standard acid electrolyte whereas Table 2 shows the values of the Tafel slope, exchange current (i_o) and the hydrogen overpotential. From the Tafel slopes, it can be inferred that the hydrogen evolution mechanism is similar for all the electrolytes studied. On the other hand, colloidal silica electrolytes present lower hydrogen overpotential and, in some cases, higher i_o, probably due to the higher iron content as impurity of these compounds, whereas fumed silica compounds present a behaviour similar to the acid electrolyte. This fact can seriously affect the water consumption performance of the gel batteries [14]. Finally in the linear voltammetry (anodic sweep) of the PbO_2 WE, the results obtained show a similar behaviour for all the electrolytes tested.

Electrochemical impedance spectroscopy measurements were carried out to study the influence of the electrolyte morphology on the battery performance [15]. Preliminary results are shown in Figs. 6 and 7 where the Nyquist plots for a 18 Ah battery with acid and gel (Silica Compound A, 6%) are represented. Impedance spectra were recorded during the battery discharge at the C/10 rate, so that Nyquist plots were obtained at different states of charge (SOC). Spectra from both systems show similar shapes: an inductive part, an ohmic resistance, two capacitative semi-circles and a Warburg impedance. Gel batteries present higher ohmic resistance than flooded batteries. The diffusional part of the signal appears at higher frequencies in gel batteries than in flooded batteries: in fact, in flooded batteries the Warburg impedance does not appear till very low SOC [12,16].

These results reveal the importance of the three dimensional structure created by the silica, on the diffusional battery processes. According to these results, a decrease in the capacity and in the high rate performance is expected when using gel with regard to the standard flooded battery.

3.2. Battery testing

To check the cycling performance of different gel electrolyte compositions in batteries, modules rated 12 V/18 Ah, with five positive and five negative electrodes per cell and resin leaf separators, were assembled.

Prototype series were filled with different gel electrolytes using commercial additives and sulphuric acid 1.300 g cm^{-3}. In order to compare this technology with the standard flooded

Table 2
Initial potential of H_2 evolution, Tafel slope and exchange current for different silica based gelators

	Initial potential of H_2 evolution versus MSE (V)	TAFEL slope	Exchange current i_o (A cm^{-2})
Sulphuric acid (1.285 g cm^{-3})	−1.60	−0.19012	4.96×10^{-9}
F (6%)	−1.40	−0.19286	3.21×10^{-8}
G (6%)	−1.35	−0.16444	4.24×10^{-9}
E (6%)	−1.60	−0.1918	5.44×10^{-9}

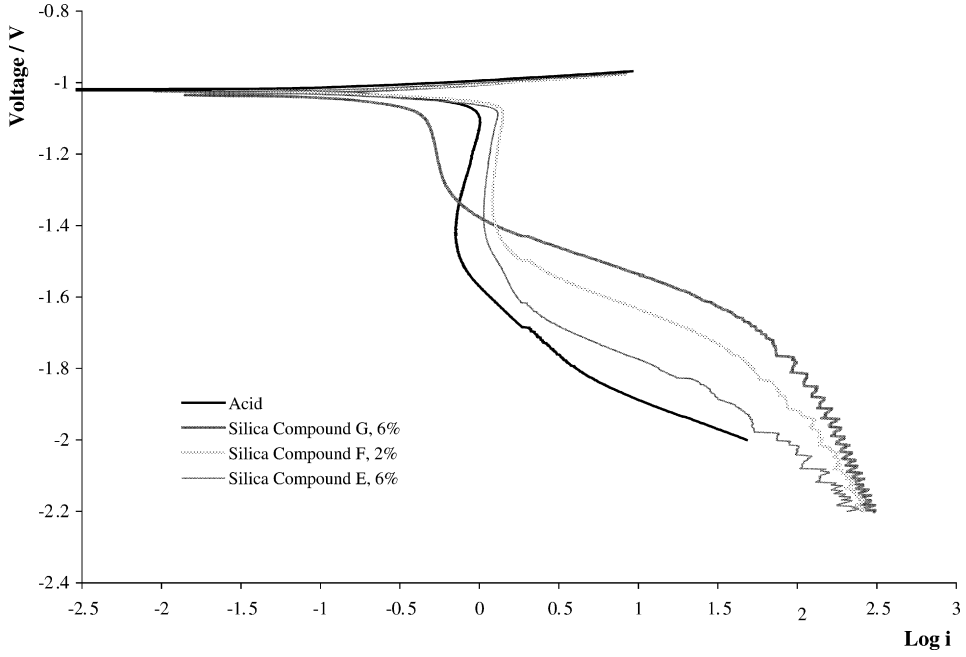

Fig. 5. Tafel plots of a Pb WE in different electrolytes. Cathodic sweep.

batteries, some batteries were filled only with sulphuric acid. Gel batteries with the standard and with the special AGM design, besides the flooded batteries, were tested according to the same test protocol.

The initial electrical test results are summarised in Table 3. The use of gel electrolytes provokes a reduction of the discharge capacity [8,12]: a 5–15% decrease at the C/20 rate and a 10–28% decrease in the 25 A discharge (reserve capacity). This effect is not appreciated in gel batteries with the AGM design, probably due to the special battery design optimised for high power applications (eight positive and seven negative electrodes per cell) and to the use of colloidal silica formulations with a very open structure.

Concerning the high rate and cold cranking performances, the main important difference is observed between batteries with resin and with AGM separator. As it was expected, AGM

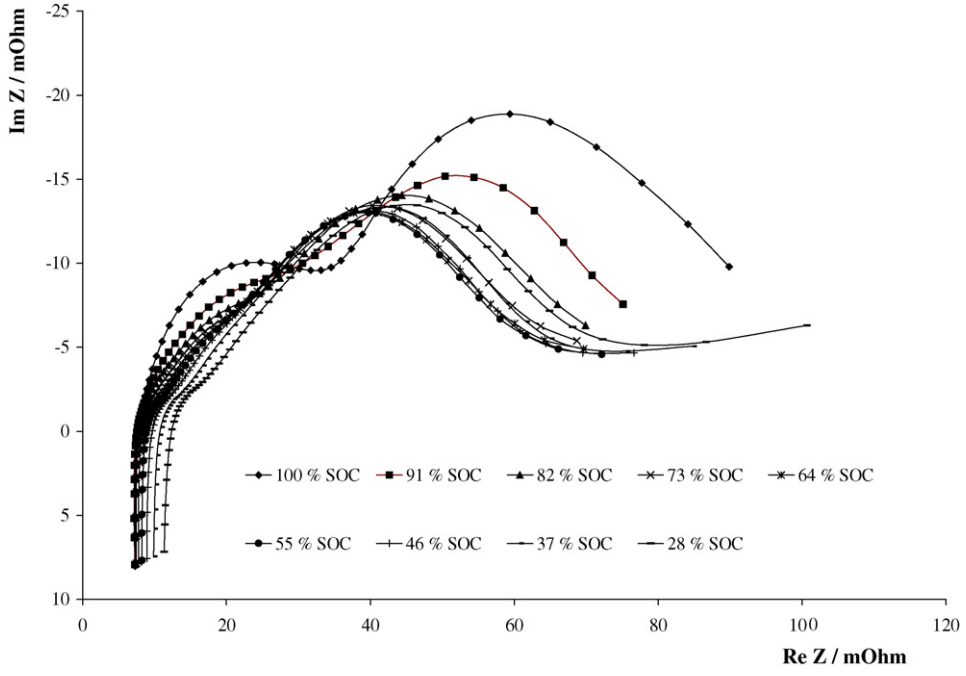

Fig. 6. Nyquist plot of a 18 Ah flooded lead acid battery.

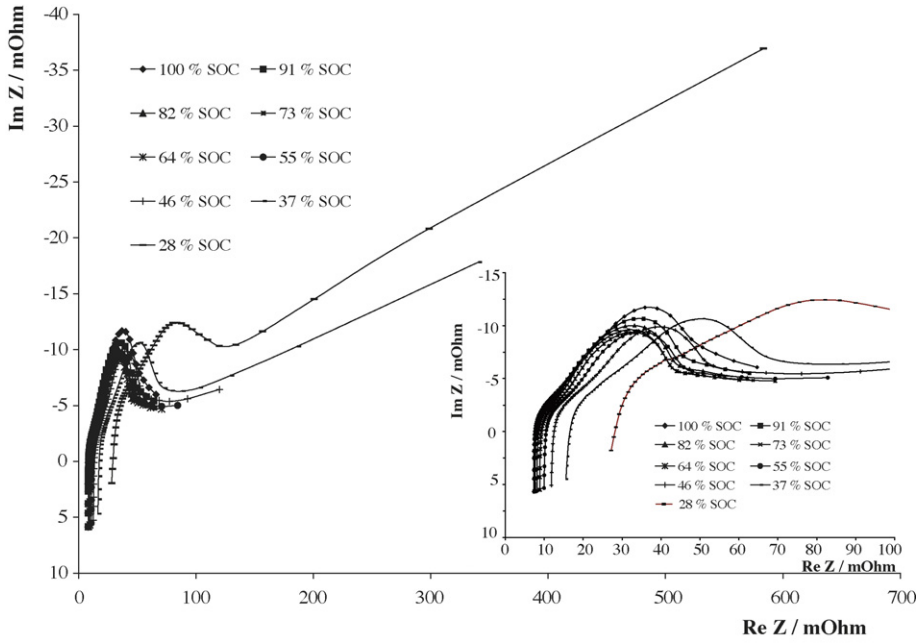

Fig. 7. Nyquist plot of a 18 Ah gel VRLA battery.

Table 3
Initial electrical test results of 12 V batteries with different electrolyte formulations

Electrolyte formulation	Capacity (Ah) (0.9 A to 10.5 V, 25 °C)	Reserve capacity (min) (25 A to 10.5 V, 25 °C)	High rate discharge, time (9 V) (min), (100 A to 9 V, 25 °C)	Cold cranking voltage (10 s) (V), time (7.2 V) (s) (200 A to 7.2 V, −18 °C)
H_2SO_4	20.7	29.3	4.3	8.13–45
A (6%)	19.3	26.4	4.8	8.03–44
B (4%)	17.8	24.5	4.1	7.93–41.5
C (4%)	18.5	26.3	4.2	7.99–43
F (1.5%)	19.8	24.5	3.8	8.13–39
F (2%)	18.6	25.2	4.0	7.86–38
F (3%)	18.6	24.1	3.5	7.32–17
G (5.3%)	18.7	23.5	3.6	7.38–15
G (6%)	18.1	24.3	3.7	7.39–17
E (4%)	17.6	24.5	3.6	7.82–34
D (5%)	17.8	25.6	4.1	7.93–39
H_2SO_4 (AGM)	18.7	28.2	NA	NA
F (1%, AGM)	17.6	30.1	5.3	9.39–58.5
G (3%, AGM)	17.5	29.2	4.5	9.35–52

batteries with thinner electrodes present better performance than the standard design, and no significant differences are detected when adding a gel electrolyte with regard to the same battery design filled with acid. On the other hand, standard gel batteries show, in most cases, lower performances than standard batteries filled only with acid. For a same gelator used, the internal resistance increases at higher silica content in the electrolyte.

Cycle life performance of the different prototypes presents important differences (Table 4). As it was expected, batteries filled with acid led to much shorter cycle life at the C/3 rate and 50% SOC, 17.5% DOD conditions than gel batteries [17,18]. Comparing colloidal and fumed silica battery performances during the cycle life test, an important capacity decrease is observed for the former throughout the test (Fig. 8).

Table 4
Cycle life test of 12 V gel batteries with commercial additives (17.5% DOD, 50% SOC, C/3 rate)

Gel formulation	No. cycles
A (6%)	4505
A (4%)	2805
B (4%)	2125
E (6%)	850
H_2SO_4	255
F (1.5%)	850
F (2%)	850
F (3%)	1870
F (1%, AGM design)	1785
G (3%, AGM design)	3400
G (5.3%)	850
G (6%)	1020

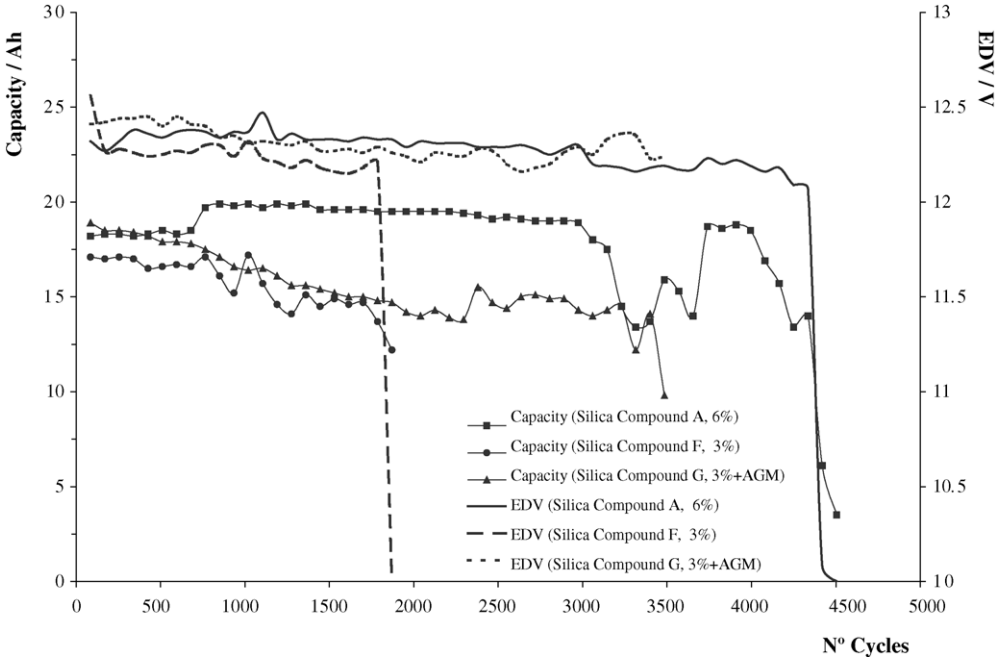

Fig. 8. Capacity and end discharge voltage evolution during low-moderate rate PSOC cycle life test for colloidal and fumed silica gel batteries.

In order to check the effect of the lower hydrogen overpotential detected in the Tafel studies, the water loss has been measured during the cycle life test. The highest water consumption is found in the colloidal gel batteries, confirming the Tafel results. On the other hand, in all the cases, most of the water consumption is observed at the beginning of the cycling. When the battery reaches its saturation level (enough cracks in the gel), the recombination efficiency increases and the water consumption is stabilised.

Finally, batteries with 6% Silica Compound A have been tested according to the Stop and Start cycling profile shown in Fig. 1. Fig. 9 shows the end of discharge voltage and the recharged capacity every 500 microcycles for a battery tested according to Test 1 in Table 5. In these conditions, more than 80,000 microcycles were completed whereas the same battery design failed after 4000 microcycles in the same cycling profile without the extra recharge. Visual inspection during tear-down analysis of the batteries operated without extra

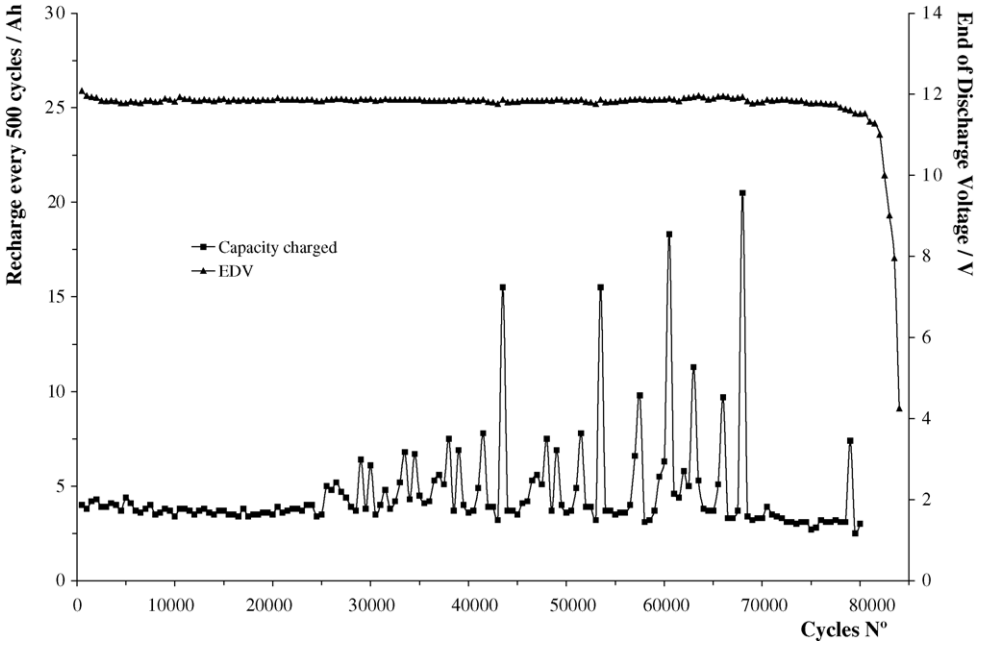

Fig. 9. Capacity recharged every 500 cycles and end of discharge voltage of batteries tested according to Stop and Start profile.

Table 5
Stop and Start testing profiles

Test	Microcycle	Key life test
1	Charge (30.9 A/16 V/20 s) Discharge (30 A/40 s) Charge (30.9 A/16 V/40 s) Discharge (30 A/20 s)	500 microcycles, recharge (30 A/16 V/1 h), air draught cooling
2	Charge (30.9 A/16 V/20 s) Discharge (30 A/40 s) Charge (30.9 A/16 V/40 s) Discharge (30 A/20 s)	500 microcycles, recharge (30 A/16 V/1 h), ambient temperature
3	Charge (30.9 A/16 V/20 s) Discharge (30 A/40 s) Charge (30.9 A/16 V/40 s) Discharge (30 A/20 s)	500 microcycles, recharge (30 A/16 V/1 h), rest (6 h 20 min)
4	Charge (30.9 A/16 V/20 s) Discharge (30 A/40 s) Charge (30.9 A/16 V/40 s) Discharge (30 A/20 s)	100 microcycles (5×), rest 1 h(5×), recharge (30 A/16 V/1 h), rest (1 h 20 min)
5	Charge (30 A/16 V/25 s) Discharge (30 A/40 s) Charge (30 A/16 V/50 s) Discharge (30 A/20 s)	500 microcycles, rest (5 h 15 min)

recharge showed strong sulphation of electrodes due to poor recharge conditions.

Records of the Ah recharged every 500 microcycles showed an increased charge acceptance along battery ageing: when the battery operates under a good "state of health", the Ah recharged remain constant (4 Ah approx.), however, when the battery ages due to irreversible sulphation processes, the battery apparently accepts more charge, even though the battery working voltage remained constant along cycling. Moreover, the capacity checks every 10,000 microcycles showed a significant capacity loss during cycling.

Other possible testing sequences with the same microcycle profile have been proposed to check the effect of battery warming (previous tests were carried out with air draught cooling, the new ones at 25 °C ambient temperature) and test pauses simulating long vehicle stops when not used. Testing conditions are summarised in Table 5.

Concerning the water loss during cycling, the tendency is similar in all the cases, however the lowest values were observed in Stop and Start 4 (resting periods every 100 microcycles + recharge) whereas the highest water loss was measured in Stop and Start 5 (recharge duration in each microcycle increased 25%, that possibly led to battery dry-out). Moreover, the internal resistance of the batteries throughout cycling increased slightly, except in those batteries that performed the Stop and Start 5 profile, which reached 20 mΩ.

The results of these cycling tests show that the eventual recharge of the battery during vehicle operation in suburban areas can allow to maintain the battery SOC. Moreover, when a rest period is included throughout the cycle life test, the battery working voltage (EDV) decreases but test duration is improved. Finally it was observed that during cycling, the temperature remains approximately constant, and increases at the end of the life, what might lead to thermal runaway processes.

3.3. Failure mode analysis

In order to determine the failure mode of the gel batteries, prototypes were recharged, torn down and, besides visual inspection, physical-chemical analyses of active materials was carried out, as PbO_2 and $PbSO_4$ contents and specific surface and porosimetry can provide valuable information about the different ageing mechanisms during cycling.

Table 6 summarises the analysis results of gel battery prototypes (Silica Compound A, 6%), tested according different procedures: the cycle life test at C/3 rate, 17.5% DOD and 50% SOC, the Stop and Start life test (at 2C rate, 2% DOD and 80% SOC) and a similar battery after only two capacity tests at the C/20 rate.

In the two cycled batteries, positive electrodes show similar sulphate content, comparable to the electrodes of the non-cycled battery. However, a slight increase in the porosity (from 51.5 to 62.8%) is observed in the battery cycled at low-moderate rate (C/3) and PSOC (50% SOC, 17.5% DOD), fact that leads to a decrease in the active mass efficiency, due to a loss of contact between particles [19].

Concerning negative plates, both cycled batteries present higher lead sulphate contents than non-cycled batteries, due to irreversible sulphation of active materials. Moreover, sulphate distribution is quite different in both cases: batteries tested according to the Stop and Start profile (moderate-high rate and shallow cycling at high SOC) show the highest sulphate concentration in the upper part of the negative plates

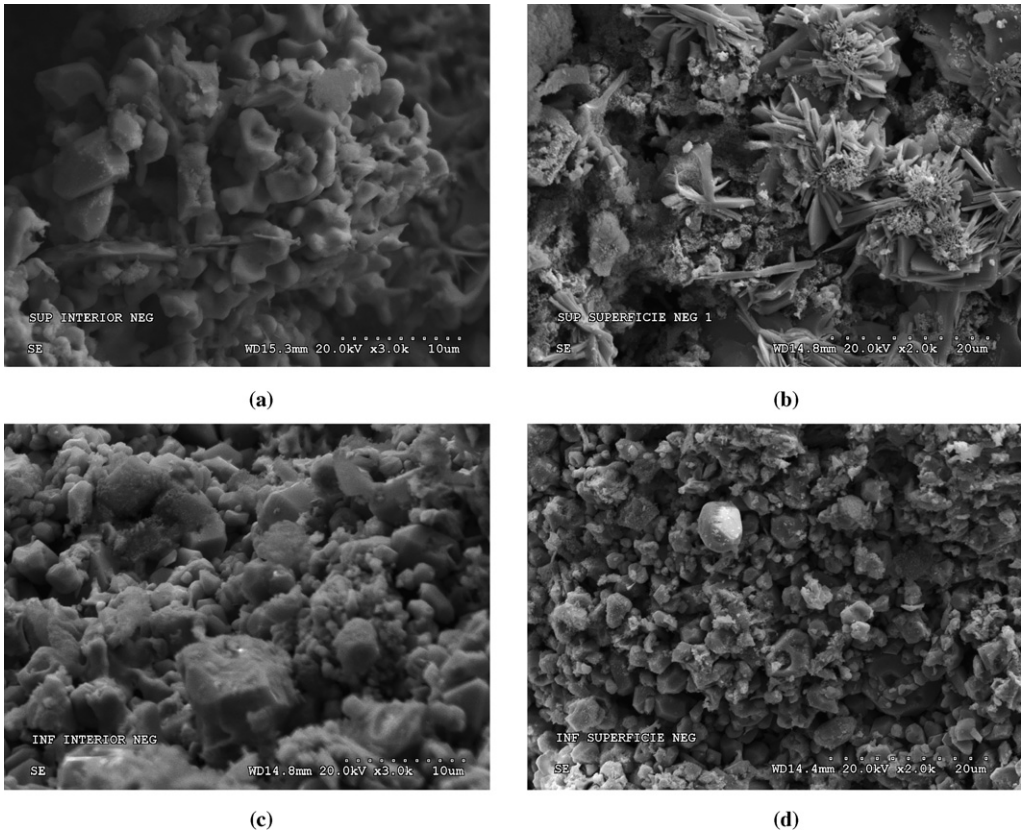

Fig. 10. SEM Micrograph of negative plates from 12 V, 18 Ah batteries filled with 6% Silica Compound A-based electrolyte, after cycling at C/3 rate, 50% SOC and 17.5% DOD: (a) upper part—inner area, (b) upper part—surface area; (c) bottom part—inner area; (d) bottom part—surface area.

whereas in the batteries aged according to the low-moderate rate, moderate cycling and lower SOC, the highest concentration of irreversible sulphates is located in the lower part of the negative electrodes. Moreover, in both cases, the irreversible sulphates are accumulated mainly on the surface of the negative plates [20].

This fact has been confirmed in the morphological analysis carried out with a scanning electron microscope (SEM). Figs. 10 and 11 show SEM images of the upper and bottom parts of the negative plates, both of the electrode surface and of the inner area. In these pictures, it can be observed that, in both cycling profiles, the larger polyhedral sulphate crystals are distributed mainly on the surface of the electrodes.

Besides the moderate irreversible sulphation of the negative plates, significant corrosion of the positive grids was also observed that limits the electrical conductivity of the positive plates.

Table 7 shows the analysis results of gel batteries with different electrolyte formulation and battery technologies (resin separator and AGM separator), tested under moderate depth of discharge (DOD) and PSOC conditions.

Negative plates from the different groups of batteries show similar characteristics than those found in gel batteries (Silica Compound A, 6%) tested according to the same testing profile and included in Table 6. An important difference is the higher specific surface of the negative active mass, when a colloidal silica is used (only resin separator design). This effect has been checked in more than 12 batteries with a specific surface increase in the range 22%–370% (170% average) and has been assigned to the access of the small silica particles into the active material creating a more open structure.

Concerning the positive plates, a higher sulphate content is detected in the positive active mass of gel batteries containing colloidal silica, due to the presence of micro short-circuits

Table 6
Chemical composition, specific surface and porosity of negative and positive plates of VRLA batteries with gel electrolyte (Silica Compound A, 6%) after different ageing conditions

Electrical test	Negative plates		Positive plates			
	$PbSO_4$ (%)	BET ($m^2\ g^{-1}$)	PbO_2 (%)	$PbSO_4$ (%)	Porosity (%)	BET ($m^2\ g^{-1}$)
Capacity test	3.5	0.52	94.6	<0.3	51.5	2.72
Cycle life test (17.5% DOD)	8.0 (T), 35.9 (B)	0.36 (T), 0.32 (B)	91.9	3.2	62.8	1.39
Cycle life test (Stop and Start)	25.5 (T), 7.6 (B)	0.30 (T), 0.30 (B)	94.8	0.5	55.9	1.69

T: top, upper part of the electrode. B: bottom, lower part of the electrode.

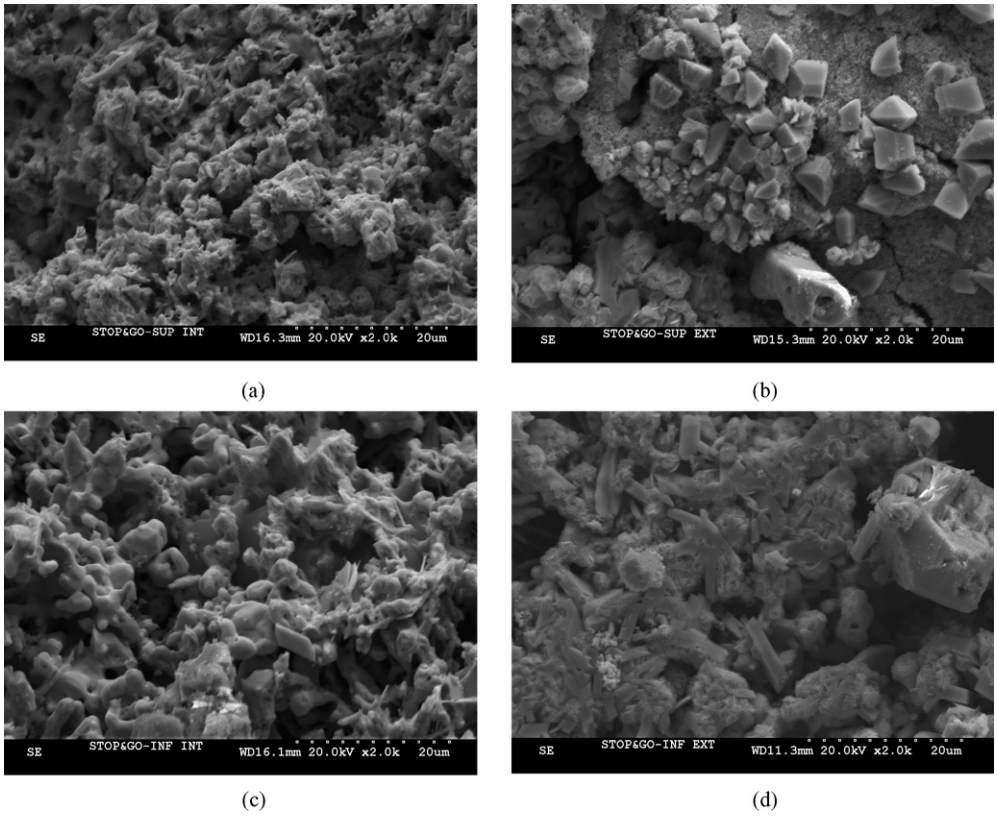

Fig. 11. SEM Micrograph of negative plates from 12 V, 18 Ah batteries filled with 6% Silica Compound A-based electrolyte, after Stop and Start cycling (2C rate, 80% SOC and 2% DOD): (a) upper part—inner area; (b) upper part—surface area; (c) bottom part—inner area; (d) bottom part—surface area.

Table 7
Chemical composition, specific surface and porosity of negative and positive plates of VRLA batteries with different gel electrolytes after cycle life test (17.5% DOD, 50% SOC)

Electrolyte formulation	Negative plates		Positive plates			
	$PbSO_4$ (%)	BET ($m^2\ g^{-1}$)	PbO_2 (%)	$PbSO_4$ (%)	Porosity (%)	BET ($m^2\ g^{-1}$)
1% F (AGM)	12.3 (T), 31.5 (B)	0.33 (T), 0.30 (B)	88.9	5.4	56.2	2.84
3% G (AGM)	47.8 (T), 52.1 (B)	0.36 (T), 0.40 (B)	82.6	13.6	53.8	1.83
6% E	2.1 (T), 10.0 (B)	0.37 (T), 0.37 (B)	94.0	1.4	58.3	2.10
5% D	5.9 (T), 18.6 (B)	0.36 (T), 0.34 (B)	91.9	4.0	57.9	2.03
3% F	9.7 (T), 24.6 (B)	0.49 (T), 0.58 (B)	83.3	12.7	59.5	2.15
6% G	2.5 (T), 18.9 (B)	1.38 (T), 1.38 (B)	88.2	7.2	57.5	3.40

T: top, upper part of the electrode. B: bottom, lower part of the electrode.

generated by lateral plate growth, and the use of leaf separators. Fumed silica based electrolytes maintain the structure throughout battery operation whereas colloidal silica based electrolytes lose the gel strength along cycling. In this way, the stable solid structure of the fumed silica electrolytes prevents the short-circuit formation and, finally, batteries fail due to positive grid corrosion.

4. Conclusions

Different gel formulations have been studied from a kinetic and an electrochemical point of view, for VRLA batteries for advanced automotive applications. 18 Ah 12 V batteries have been assembled and filled with those electrolyte formulations that showed the best combination of gel processing and hardness properties. As expected, initial battery performance, specially high rate discharges and cold cranking, is poorer with gel electrolyte when compared with standard sulphuric acid. However, this effect can be minimised with some design modifications, such as thinner electrodes, reduced interplate distance and the use of low electrical resistance separator materials.

Ageing tests of the batteries were carried out under two different PSOC procedures, one characterised by low-moderate rate (C/3) and moderate DOD (17.5%) and the other with a moderate-high rate (2C), shallow DOD (2%) and higher SOC (80%), the latter simulating battery working conditions in a

vehicle equipped with Stop and Start function. In both cases results are quite satisfactory.

Tear-down analysis of batteries after the ageing tests showed significant corrosion of positive grids as well as moderate sulphation of the negative plates, located mainly on the bottom part of the plates, in the batteries tested at low-moderate rate and 17.5% DOD-50% SOC and on the upper part after the Stop and Start cycling test.

Acknowledgements

This project is being partially funded by the European Commission, under the Energy, Environment and Sustainable Development Programme, ENERGIE Contract no. ENK6-CT-2002-00630.

References

[1] D. Berndt, J. Power Sources 100 (2001) 29–46.
[2] P.T. Moseley, D.A.J. Rand, J. Power Sources 133 (2004) 104–109.
[3] R. Knorr, A. Schwake, M. Soria, H. García, M. Reimerink, D. Macerata, M. Ullrich, Proceeding of the ELEDrive Transportation Conference, Estoril (Portugal), 2004.
[4] M. Anderman, J. Power Sources 127 (2004) 2–7.
[5] N. Sato, Proceedings of the Third International Advanced Automotive Battery Conference, Nice, June 2003. Session 3A, paper 11.
[6] R. Wagner, in: D.A.J. Rand, P.T. Moseley, J. Garche, C.D. Parker (Eds.), Valve-regulated Lead-Acid Batteries, Elsevier, Amsterdam, 2004, p. 447.
[7] Improved Energy Supply for the Integrated Starter Generator with Double Layer Capacitor and Energy Battery for Cars with 42V (SUPERCAR), ENERGIE contract ENK6-CT-2002-00630.
[8] D.W.H. Lambert, P.H.J. Greenwood, M.C. Reed, J. Power Sources 107 (2002) 173–179.
[9] M.L. Soria, J. Valenciano, A. Ojeda, J. Power Sources 136 (2004) 371.
[10] M.L. Soria, J.C. Hernández, J. Valenciano, A. Sánchez, F. Trinidad, J. Power Sources 144 (2005) 473–485.
[11] M.P. Vinod, A.B. Mandle, S.R. Sainkar, K. Vijayamohanan, J. Appl. Electrochem. 27 (1997) 462–468.
[12] L. Wu, H.Y. Chen, X. Jiang, J. Power Sources 107 (2002) 162–166.
[13] K. Dash, K. Bose, Bull. Electrochem. 2–4 (1986) 387–390.
[14] M.P. Vinod, K. Vijayamohanan, S.N. Joshi, J. Power Sources 70 (1998) 103–105.
[15] E. Karden. PhD. thesis. RWTH, Aachen, 2001.
[16] M.P. Vinod, K. Vijayamohanan, J. Power Sources 89 (2000) 88–92.
[17] H. Tuphorn, J. Power Sources 40 (1992) 47–61.
[18] H. Tuphorn, J. Power Sources 46 (1993) 361–373.
[19] J.H. Yan, W.S. Li, Q.Y. Zhan, J. Power Sources 133 (2004) 135–140.
[20] L.T. Lam, N.P. Haigh, C.G. Phyland, A.J. Urban, J. Power Sources 133 (2004) 126–134.